THE ASTROPHYSICAL JOURNAL, 461:465–471, 1996 April 10

ELECTRON TEMPERATURE AND EMISSION MEASURE DETERMINATIONS OF VERY FAINT SOLAR FLARES

U. FELDMAN AND G. A. DOSCHEK
Code 7608, E. O. Hulburt Center for Space Research, Naval Research Laboratory, Washington, D.C. 20375-5352
AND
W. E. BEHRING
Code 682, Goddard Space Flight Center, Greenbelt, MD 20771
Received 1995 February 22; accepted 1995 October 13

ABSTRACT

We have studied 28 flares in the X-ray magnitude range of A2–A9 using high-resolution Bragg crystal spectrometer data obtained from instrumentation flown on the *Yohkoh* spacecraft. Flares in the A-class category can be detected in spectral lines of He-like ions formed at low temperatures. Their average temperature is approximately 5×10^6 K, and their emission measure as determined from the S XV resonance line near 5 Å varies between 2×10^{46} and 1×10^{48} cm^{-3}.

Subject headings: Sun: flares — Sun: X-rays, gamma rays

1. INTRODUCTION

The *Geostationary Operational Environmental Satellite* (*GOES*) 1–8 Å detector is one of several instruments used for monitoring flare activity on the Sun's surface. Seen by the *GOES* 1–8 Å detector, the flare output varies in time with a characteristic behavior that is similar for most flares. Schematically, the 1–8 Å intensity versus time can be characterized by a phase of monotonically increasing intensity, a maximum phase, and a phase of declining intensity, in which the rise phase and often the decay phase can be approximated by exponentials (e.g., Feldman, Doschek, & McKenzie 1984; Feldman et al. 1995). The maximum intensities and the *e*-folding times of the rise and decay phases vary considerably from flare to flare. The peak flux recorded at Earth by the 1–8 Å *GOES* detector is used to rank the flare's X-ray magnitude on a logarithmic scale. The most intense solar flares, designated as X-ray magnitude X, emit peak fluxes greater than 10^{-4} W m^{-2}. Flares emitting peak fluxes of 1×10^{-4} W m^{-2} are assigned an X-ray magnitude of X1, while those emitting peak fluxes of 2×10^{-3} are assigned an X-ray magnitude of X20. The faintest flares classified by the *GOES* 1–8 Å detector are in the range of $1–9 \times 10^{-8}$ W m^{-2}. They are designated with X-ray magnitudes of A1–A9. Examples of the relationship between 1–8 Å fluxes and X-ray classes are shown in Figure 1.

The *GOES* 1–8 Å detector emission from individual flares is superimposed on a background emission. The average flux in the background emission changes according to solar activity levels. When the general level of activity is very high, as was the case on 1991 October 23 (see Fig. 1), the background flux reached levels of $\approx 2 \times 10^{-6}$ W m^{-2}. At such times, all flares having fluxes smaller than about 1×10^{-6} W m^{-2} are concealed in the background emission. However, during quieter periods, as was the case on 1994 June 22 (see Fig. 1) when solar activity was significantly reduced, background levels may be as low as 1×10^{-8} W m^{-2}. During such periods, flares having X-ray magnitudes in the A2–A9 range are detectable and can be studied with sufficiently sensitive instruments.

In the past, most research was directed toward brighter X-ray magnitude X- and M-class flares, with somewhat less emphasis on C-class flares. In this paper, we discuss the electron temperature and emission measure variations in plasmas generated by A2–A9 class flares, which are the smallest flares detected by the *GOES* X-ray detectors. The temperatures and emission measures are determined from a high-resolution Bragg crystal spectrometer.

2. THE EXPERIMENT

The Japanese satellite *Yohkoh* (Ogawara et al. 1991) was launched on 1991 August 30. During its first 3 years of operation, it has observed many hundreds of flares. The *Yohkoh* instruments consist of a soft X-ray telescope, a hard X-ray telescope, a wide-band X-ray to gamma-ray spectrometer package, and a Bragg Crystal Spectrometer package (BCS). Actual observations started in 1991 October when the activity of solar cycle 22 was still very high (see Fig. 1).

The BCS is described in detail by Culhane et al. (1991). Briefly, four bent Ge crystals diffract radiation in four narrow wavelength ranges. Uncollimated solar X-rays are incident on each crystal, and the reflected radiation passes through a window of a sealed proportional counter with one-dimensional position encoding. The position encoding is achieved by a wedge-and-wedge readout. Because the germanium crystals are bent, the Bragg diffraction condition is satisfied for different wavelengths at different locations along the crystal length, so that the detector simultaneously records a complete spectrum covering a small wavelength region. Photon counts are accumulated into bins of either 128 or 256 wavelengths. There are systems for rejecting background counts and for sensing X-ray count rate increases to enable data readout modes to be changed if desired.

The four wavelength channels cover intervals around the Lyman-α lines of Fe XXVI (1.78 Å) and the resonance lines (transition $1s^2\,{}^1S_0$–$1s2p\,{}^1P_1$, or line w in the notation of Gabriel 1972) of the helium-like ions Fe XXV, Ca XIX, and S XV (wavelengths 1.85 Å, 3.18 Å, and 5.04 Å, respectively). In the usual flare mode, a complete four-channel spectrum is recorded once every 3 s.

As will be shown later, the electron temperatures of plasmas generated by flares having X-ray magnitudes of A2–A9 are seldom higher than 8×10^6 K. Thus, Fe XXV or Ca XIX emission is not detected from A-class flares. In con-

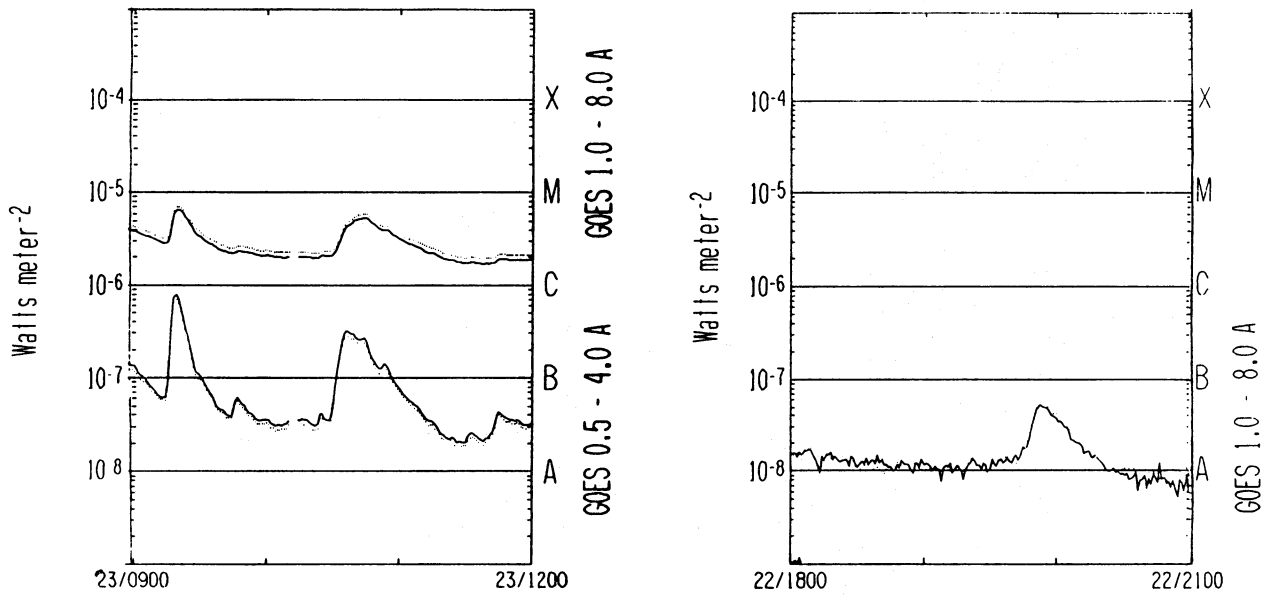

FIG. 1.—Sections of records of X-ray and optical data obtained by the *GOES* 1–8 Å detectors, consisting of emission from flares and from background radiation during periods of high (1991 October 23) and low (1994 June 22) solar activity.

trast, at such low temperatures, line ratios of S XV and the nearby satellites are quite prominent and can serve as efficient electron temperature and emission measure indicators. Studies described in this paper are based on BCS measurements obtained by the BCS S XV channel.

The S XV channel covers the 5.01–5.11 Å wavelength range, which includes the following four prominent S XV lines: 5.0387 Å $1s^2\,{}^1S_0$–$1s2p\,{}^1P_1$ (line w), 5.0631 Å $1s^2\,{}^1S_0$–$1s2p\,{}^3P_2$ (line x), 5.0665 Å $1s^2\,{}^1S_0$–$1s2p\,{}^3P_1$ (line y), and 5.1015 Å $1s^2\,{}^1S_0$–$1s2s\,{}^3S_1$ (line z). At fairly high temperatures $T_e \geq 1.0 \times 10^7$ K, the emission in the S XV channel comes primarily from these four lines. However, as the temperature decreases, S XIV lines, which are formed by dielectronic recombination and by inner shell excitation, also become prominent. The most prominent among the dielectronic recombination lines, the 5.0968 Å $1s^22p\,{}^2P_{1/2}$–$1s2p^2\,{}^2D_{3/2}$ (line k) and the 5.1014 Å $1s^22p\,{}^2P_{3/2}$–$1s2p^2\,{}^2D_{5/2}$ (line j), are nearly blended with the S XV line z, while the most prominent among the inner shell excitation lines, the 5.0855 Å $1s^22s\,{}^2S_{1/2}$–$1s2s2p\,{}^2P_{3/2}$ and the 5.0875 Å $1s^22s\,{}^2S_{1/2}$–$1s2s2p\,{}^2P_{1/2}$ lines, are well separated (see Fig. 2).

The relative intensities of the S XV and S XIV lines are temperature sensitive and are used to deduce our temperatures for X-ray magnitude A-class flares. The temperature sensitivity is approximately of the form $I_s/I_w \propto T_e^{-1}$, where I_s is the intensity of a satellite line and I_w is the intensity of the S XV resonance line. Figure 2 shows theoretically calculated spectra from several temperatures between 3.2×10^6 and 1×10^7 K, and Figure 3 shows *Yohkoh* BCS observed spectra of S XV and its satellites for the same temperatures. The theoretical spectra were calculated using a computer program written by Zarro, Lemen, & Phillips (1994) that utilizes theoretical calculations by Bely-Dubau et al. (1982a, b), (1978, 1985). Cornille & Dubau (1990), and Vainstein & Safronova (1978). Notice that the S XV spectra are most sensitive to temperature variations at temperatures lower than 6×10^6 K.

The emission measures for the X-ray magnitude A-class flares are determined from the temperature and total flux in the S XV resonance line. The flux (F_{12}) of the S XV resonance line at Earth in photons $\mathrm{cm}^{-2}\,\mathrm{s}^{-1}$ is given by

$$F_{12} = \frac{1}{4\pi R^2} \int N_g n_e C_{12}\, dV\,, \tag{1}$$

where $R = 1$ AU (in cm), N_g is the ion ground-state number density, n_e is the electron density, C_{12} is the collisional excitation rate coefficient ($\mathrm{cm}^3\,\mathrm{s}^{-1}$) of the resonance transition, and dV is the flare volume over which the emission occurs. For S XV, at flare densities the entire ion population is in the ground state N_g to a high degree of accuracy. The ground-state number density N_g can be expressed as an identity,

$$N_g = \frac{N_g}{N_E}\frac{N_E}{N_H}\frac{N_H}{n_e}\, n_e\,, \tag{2}$$

where N_g/N_E is the fractional ion abundance [which we define as $F(T_e)$] in ionization equilibrium at the electron temperature T_e, N_H/n_e is approximately 0.8, and N_E/N_H is the coronal elemental abundance which we define as A_H. For S we adopt the value $A_S = 2.1 \times 10^{-5}$, which is 1.3 times the photospheric value.

Substitution of equation (2) into equation (1) gives

$$F_{12} = \frac{0.8}{4\pi R^2} A_H F(T_e) C_{12}(T_e)(n_e^2\, \Delta V)\,, \tag{3}$$

where ΔV is the average volume of plasma at temperature T_e. We note that in equation (3), it is only justified to remove $F(T_e)$ and $C(T_e)$ from the integral in equation (1) if the plasma is isothermal at temperature T_e. In practice, this is often not the case, but usually there are not enough spectral lines available to justify a better approximation. The emission measure term, $n_e^2\,\Delta V$ in equation (3), is therefore an average value representing plasma near the temperature T_e. Equation (3) relates the emission measure to the temperature, total S XV flux, and other relevant atomic data. In practice, the temperature and emission measure are deter-

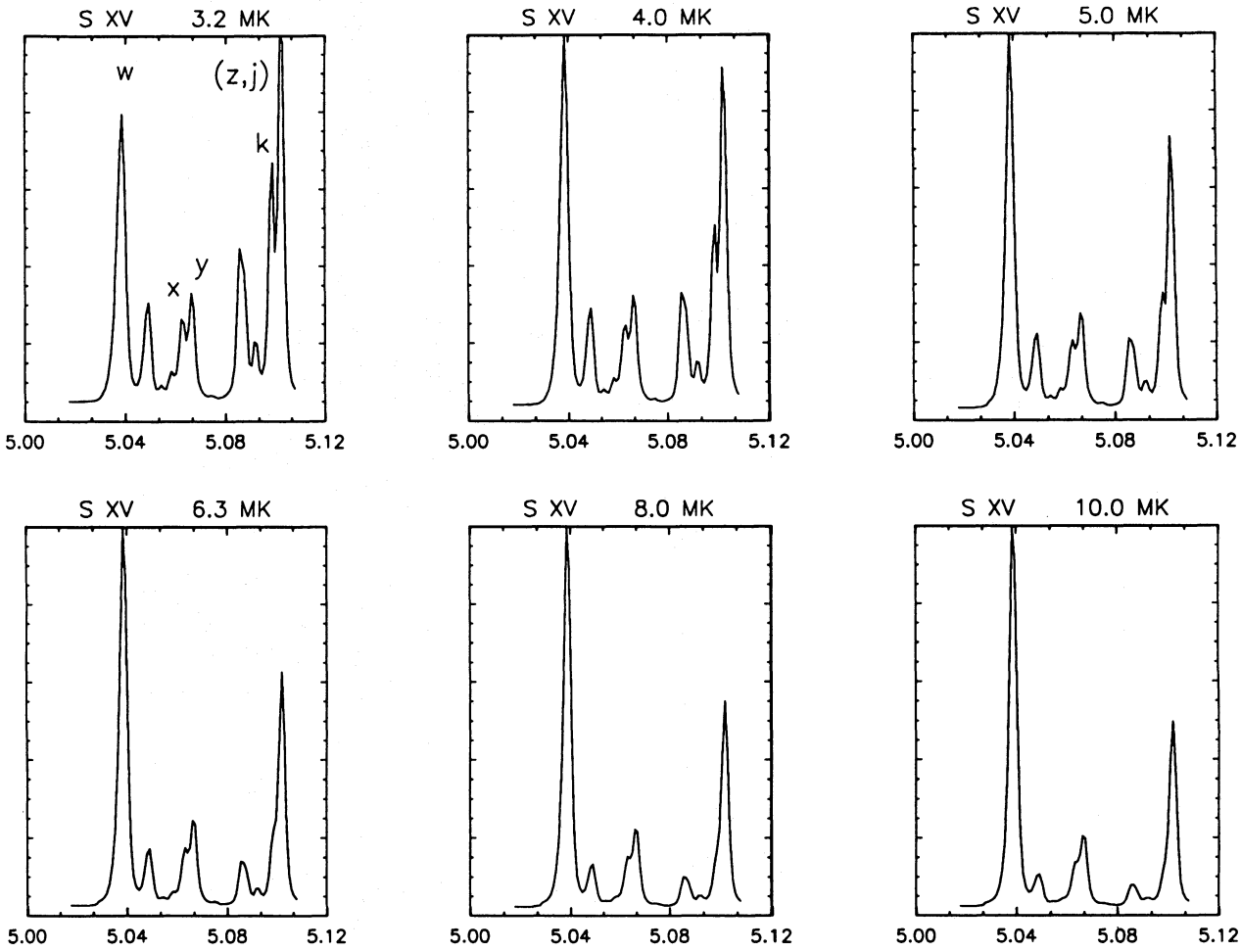

FIG. 2.—Synthetic spectra as a function of temperature in the 5.00–5.12 Å wavelength range. The spectra consist of S XV lines, i.e., 5.0387 Å $1s^2\,{}^1S_0$–$1s2p\,{}^1P_1$ (line w), 5.0631 Å $1s^2\,{}^1S_0$–$1s2p\,{}^3P_2$ (line x), 5.0665 Å $1s^2\,{}^1S_0$–$1s2p\,{}^3P_1$ (line y), and 5.1015 Å $1s^2\,{}^1S_0$–$1s2s\,{}^3S_1$ (line z), and prominent S XIV lines, i.e., 5.0968 Å $1s^22p\,{}^2P_{1/2}$–$1s2p^2\,{}^2D_{3/2}$ (line k), and 5.1014 Å $1s^22p\,{}^2P_{3/2}$–$1s2p^2\,{}^2D_{5/2}$ (line j) (from Zarro et al. 1994).

mined simultaneously from an interactive fit of synthetic spectra to actual spectra.

The product of the excitation rate coefficient $C_{12}(T_e)$ and the ionization fraction $F(T_e)$ represent the temperature dependence of the flux F_{12}, and it is often called the contribution function. Functions $[G(T_e)]$ approximately proportional to the contribution function for S XV (and also Ca XIX and Fe XXV) are shown in Figure 4. These functions represent most of the temperature dependence of the contribution function and are defined as

$$G(T_e) = F(T_e) \exp(-\Delta E/kT_e)/T_e^{1/2}\,, \qquad (4)$$

where ΔE is the resonance line transition energy. S XV values for $F(T_e)$ were obtained from Arnaud & Rothenflug (1985). S XV values of $C_{12}(T_e)$ were obtained from Cornille & Dubau (1990), using the same type of calculations as described by Bely-Dubau et al. (1982a) for Fe XXV.

As seen from the figure, the value of $G(T_e)$ for S XV rapidly declines at very low temperatures. The maximum value of $G(T_e)$ occurs at about 1.3×10^7 K, and at 5.5×10^6 K its value is already decreased by 1 order of magnitude, at 3.8×10^6 K by 2 orders of magnitude, and at 3.0×10^6 by about 3 orders of magnitude. In these low temperature regions $G(T_e)$ is a rapidly increasing function of temperature. Because of this, it is safe to assume that whenever S XV spectra of a flare indicate such a low temperature, say T_1, much less than the maximum temperature of 1.3×10^7 K, that this result implies that there is very little plasma in the flare at temperatures greater than T_1, i.e., the rapidly increasing $G(T_e)$ favors emission from the highest temperatures present in the plasma. For the hypothetical flare in question, the maximum temperature of the bulk of the flare plasma must be close to T_1. Higher temperature plasma can exist in the flare, but the emission measure of this plasma must be substantially less than the emission measure of the plasma at T_1.

3. PROPERTIES OF X-RAY MAGNITUDE A-CLASS FLARES

The *GOES* records were searched for periods of low solar activity. It was found that the 1–8 Å X-ray background did not exceed the A3 level (3×10^{-8} W m^{-2}) for several days at a time between 1994 May and November. During some of this period, flaring activity was below the A1 level; however, at other times, the Sun produced a considerable number of A-class flares. For most of the A-class flares, no measurable signal is present in records for the *GOES* 0.5–4 Å detector.

From their qualitative appearance on the 1–8 Å *GOES* records, the X-ray light curves of flares having X-ray magnitude A and the light curves of flares having X-ray magnitudes M and X look quite similar (see Fig. 1). Their output varies in time with the same characteristic behavior as

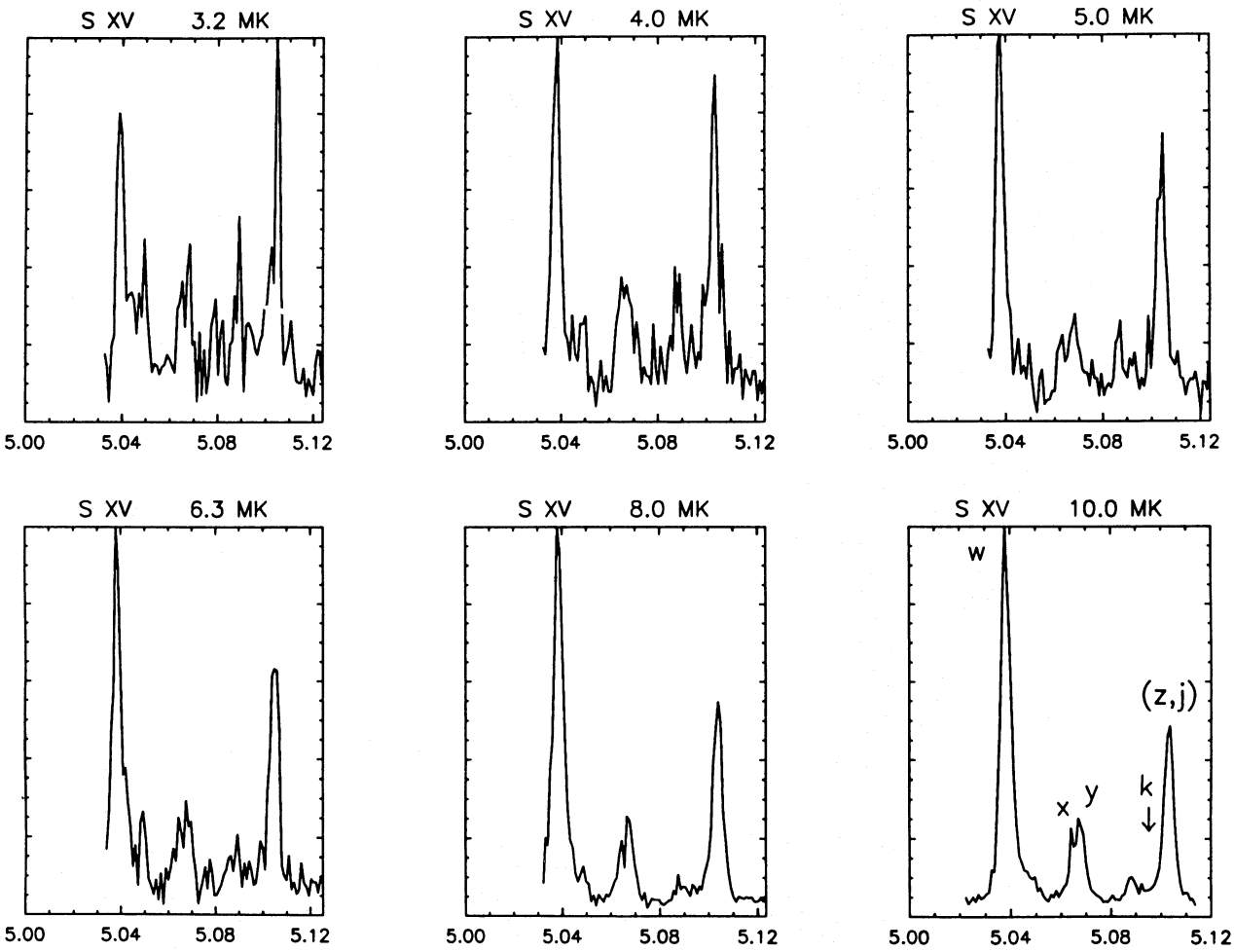

FIG. 3.—Observed BCS spectra as a function of temperature in the 5.00–5.12 Å wavelength range. The spectra consist of lines from S XV and S XIV.

described above for brighter flares. As for the brighter flares, the *e*-folding times of the rise and decay phases vary considerably from flare to flare.

Since our study was limited to X-ray magnitude A flares, and because the background levels are also in the A range, the peak intensity of the flares is at most a factor of about 5 above background. From our study we have found that the full width at half-maximum (FWHM) of the flare fluxes seen by the 1–8 Å *GOES* detector varies between 3 and 20 minutes. This behavior does not appear to be substantially different than the FWHM of brighter events.

In searching the BCS database for the low-activity period, we have identified 28 X-ray magnitude A flares having uninterrupted records of S XV spectra for the rise, the peak, and at least part of the decay phases. Spectra in the Fe XXV channel were not detected for any of the 28 flares. In a few of the flares, traces of spectra in the Ca XIX channel are present. However, the signal-to-noise ratio in the spectra is too low for any meaningful temperature analysis to be performed.

For each of the flares, spectra from the S XV channel averaged either over 24 or 48 s were extracted for a number of times in the rise phase, in the peak, and for a number of times in the decay phase. The general behavior of our derived S XV temperatures versus time for the A-class flares is similar to the temperature behavior observed for the brighter events (Sterling, Doschek, & Pike 1994; Feldman et al. 1995). At flare onset, the S XV temperature is relatively low. As the flare progresses, the temperature increases to a maximum that coincides with the flare's maximum emission. The electron temperature then declines in the decay phase. As examples, changes in electron temperature during the lifetimes of two flares that occurred on 1994 July 20 are shown in Figure 5. Although the hottest among the 28 A-class flares reaches 1×10^7 K, the maximum temperature of 19 of the flares is below 6×10^6 K, and the maximum temperature of three of the flares is below 4×10^6 K. The distribution of flares in terms of X-ray class and derived temperature is shown in Figure 6.

A list of the analyzed flares is given in Table 1. The table contains the times of maximum emission in the BCS S XV channel, the electron temperatures as determined from the S XIV to S XV line ratios, the *GOES* 1–8 Å X-ray magnitudes at the time of peak emission, and the background *GOES* level. The FWHM in minutes of the 1–8 Å fluxes are given in column (6), and the S XV emission measures are given in the last column.

The errors in the derived electron temperatures and emission measures are given as an option when using the *Yohkoh* BCS data reduction and analysis software. From inspection of the errors obtained for the data in Figure 5, we conclude that temperatures in the 8×10^6 K range are generally accurate to about 10^6 K or better, and temperatures in the 4×10^6 K range are generally accurate to about $0.2–0.6 \times 10^6$ K, depending on the count rate. This translates into about a 15% error in the emission measure near

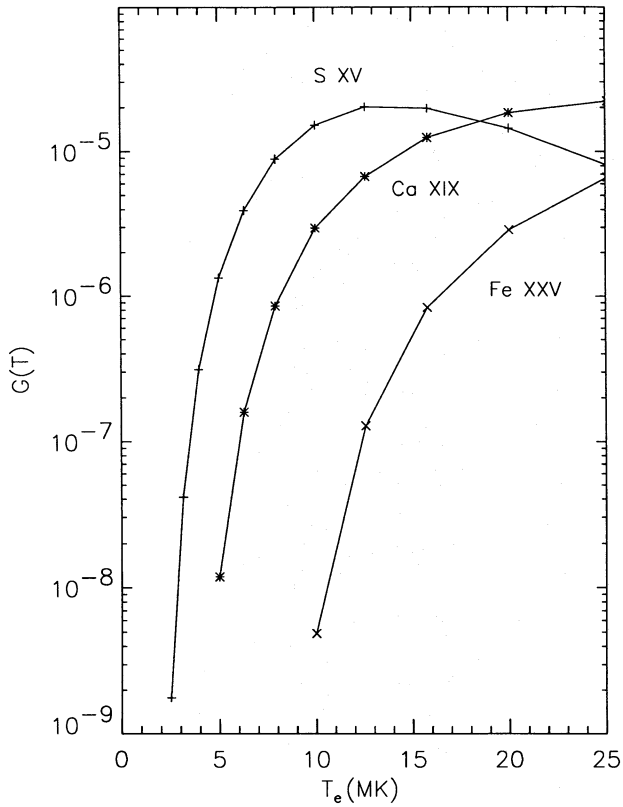

FIG. 4.—The $G(T_e)$ function vs. electron temperature for S XV, Ca XIX, and Fe XXV.

8×10^6 K and into about a 11%–60% error near 4×10^6 K. The larger emission measure errors reflect the sensitivity of the Boltzmann factors in the excitation rates at low temperatures.

The plasma electron temperature in most of the A-class flares is too low to produce He-like and H-like ions from Ar and higher Z elements which contribute substantial flux at wavelengths $\lambda \leq 4$ Å. Thus, it is not surprising that the flux from A-class flares is below the sensitivity level of the *GOES* 0.5–4 Å detector.

Figure 7 is a display of the S XV emission measure versus

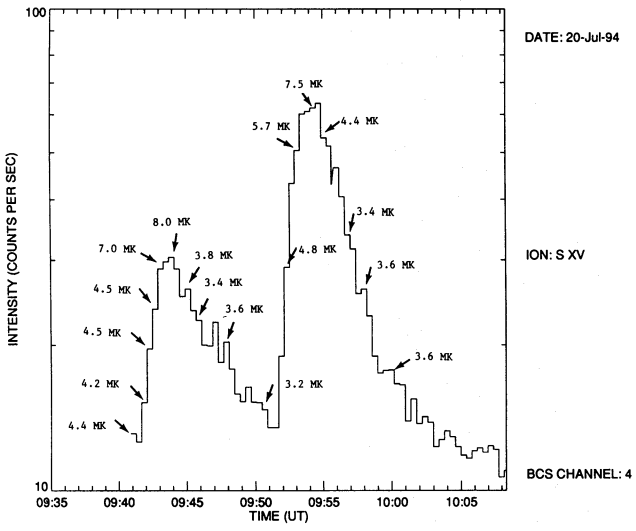

FIG. 5.—Changes in the electron temperature during the lifetime of two flares that occurred on 1994 July 20.

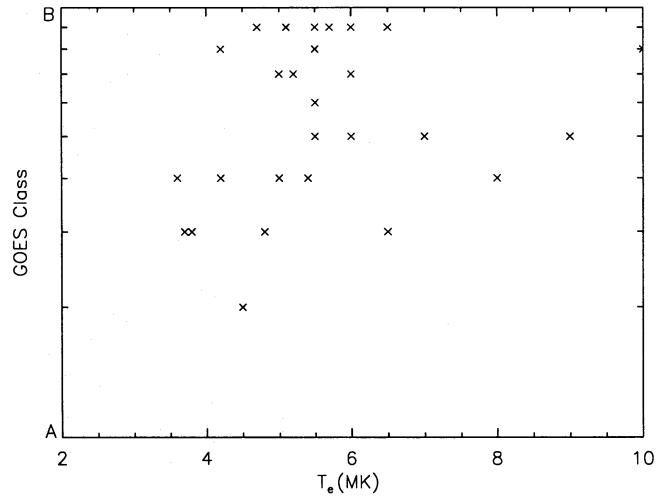

FIG. 6.—*GOES* X-ray class vs. electron temperature at peak flux for flares having X-ray classes of A2–A9.

S XV electron temperature for the 28 flares with X-ray magnitudes in the A2–A9 range. The solid line is a least-squares linear fit to the data. The observed emission measure range is approximately 2 orders of magnitude (2×10^{46} to 1×10^{48} cm^{-3}). The shape of the emission measure distribution in Figure 7 depends critically on the sensitivity of both *GOES* and BCS. For example, very cold flares ($T_e < 5 \times 10^6$ K) with emission measures in the 10^{46} cm^{-3} range are not detected by *GOES* because of the particular properties of the *GOES* 1–8 Å detector. The *GOES* 1–8 Å detector is only slightly sensitive to radiation with wavelengths $\lambda \geq 8$ Å (Donnelly & Unzicker 1974). Solar plasmas at low electron temperatures ($T_e < 5 \times 10^6$ K) emit most of their radiation at wavelengths $\lambda \geq 8$ Å. Therefore, the *GOES* 1–8 Å detector becomes increasingly less efficient to emission from plasmas with decreasing temperatures (see Fig. 8). Similarly, inspection of the $G(T_e)$ for S XV in Figure 4 shows that flares with temperatures less than about 3×10^6 K will not be detected in S XV lines because of the rapid decrease in $G(T_e)$. The 1–8 Å detector efficiency versus wavelength is reflected in the distribution of points shown in Figure 7 because only A-class flares observable with *GOES* were selected for study.

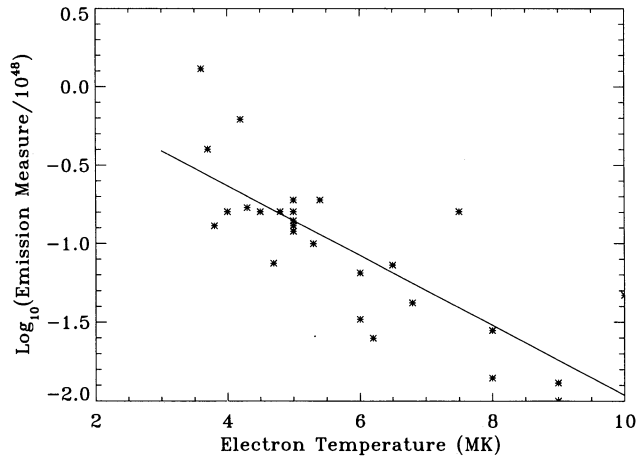

FIG. 7.—BCS S XV emission measure vs. electron temperature at peak flux for flares having X-ray classes of A2–A9. The solid line is a least-squares linear fit to the data.

TABLE 1

LIST OF ANALYZED FLARES[a]

Number (1)	Date and Time of S XV Peak Flux (2)	S XV T_e(MK) (3)	*GOES* Magnitude		FWHM (minutes) (6)	BCS Emission Measure (cm^{-3}) (7)
			Flare (4)	Background (5)		
1	May 27, 07:32	3.8	A3	A0.8	12	1.3E47
2	Jun 22, 15:06	5.4	A9	A3	17	1.9E47
3	Jun 22, 19:54	9.0	A5	A1	18	1.3E46
4	Jun 23, 03:12	3.6	A4	A2	11	1.3E48
5	Jun 23, 05:37	4.3	A4	A2	6	1.7E47
6	Jun 23, 07:25	9.0	A5	A2	8	1.0E46
7	Jun 23, 15:16	5.0	A7	A2	10	1.3E47
8	Jun 25, 01:20	8.0	A9	A2	4	2.8E46
9	Jun 25, 08:30	4.8	A9	A3	20	1.6E47
10	Jul 20, 09:44	8.0	A4	A2	4	1.4E46
11	Jul 20, 09:55	7.5	A9	A2	4	1.0E47
12	Jul 22, 15:44	6.8	A6	A3	4	4.2E46
13	Jul 26, 08:15	6.0	A5	A2	12	3.3E46
14	Jul 26, 10:24	4.7	A3	A2	6	7.5E46
15	Jul 29, 11:19	10.0	A8	A2	2	4.7E46
16	Aug 1, 05:28	4.0	A4	A2	12	1.6E47
17	Aug 2, 18:34	4.2	A8	A3	5	6.2E47
18	Aug 5, 06:36	5.0	A7	A3	3	1.4E47
19	Aug 7, 00:34	5.0	A9	A2	4	1.9E47
20	Aug 7, 00:42	5.0	A9	A2	4	1.6E47
21	Aug 27, 21:49	4.5	A3	A1	10	1.6E47
22	Aug 28, 00:49	5.0	A5	A1	17	1.4E47
23	Sep 18, 04:34	7.5	A3	A1	6	1.6E47
24	Sep 18, 12:25	3.7	A3	A2	5	4.0E47
25	Oct 2, 04:28	6.2	A2	A1	17	2.5E46
26	Nov 14, 10:09	6.0	A8	A3	7	6.5E46
27	Nov 15, 08:53	5.0	A4	A2	4	1.2E47
28	Nov 17. 04:17	5.3	A7	A2	18	1.0E47

[a] All flares occurred in 1994.

4. SUMMARY AND CONCLUSIONS

From studying 28 flares in the X-ray magnitude range of A2–A9, we have found the following:

1. A-class flares exhibit distinct rise, maximum, and decay phases. The X-ray light curves of A flares qualitatively resemble the X-ray light curves of brighter events, e.g., the *e*-folding time of the rise phase usually is smaller than the *e*-folding time of the decay phase, as for brighter flares. The intensity versus time during the rise and decay phases of A-class flares can be approximated by exponentials.

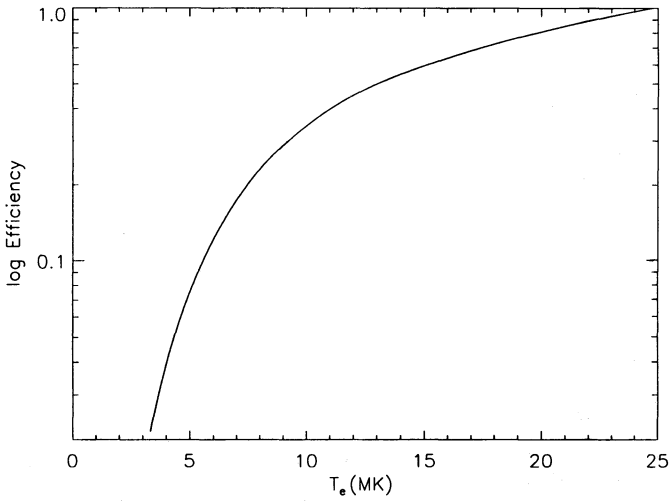

FIG. 8.—*GOES* 1–8 Å detector efficiency vs. electron temperature (from calculations in Garcia 1994).

2. A-class flares vary in electron temperatures between 1×10^7 K and less than 4×10^6 K. Their average temperature is approximately 5×10^6 K. At flare onset, the temperature is low, and as the flare progresses, the temperature increases to reach its maximum value at the time of peak emission. Once the onset of the decay phase starts, the temperature drops to a lower level.

3. The S XV emission measure varies between 2×10^{46} and 1×10^{48} cm^{-3}. The 1×10^{48} cm^{-3} value seems to be an upper limit for A-class flares with $T_e \geq 3.6 \times 10^6$ K. The value 1×10^{46} cm^{-3} appears to be a lower limit for A-class flares having temperatures of 8×10^6 to 1×10^7 K. However, because of the insensitivity of *GOES* for very low temperatures, our present study cannot establish a lower limit on emission measure for flares with $3.6 \times 10^6 \leq T_e \leq 5 \times 10^6$ K. We might be able to extend the lower limit somewhat by examining S XV flares in the BCS data base that are not present in the *GOES* data.

In this paper we have shown that the Sun produces flares having maximum temperatures as low as 3.6×10^6 K. As with the much brighter flares (Feldman et al. 1995), the spread in emission measure values of the A-class flares is also approximately 2 orders of magnitude. The maximum emission measure of flares having a maximum temperature of 1.5×10^7 K is $\approx 5 \times 10^{48}$ cm^{-3}, and the maximum emission measure of flares having a maximum temperature of 5×10^6 K is 1×10^{48} cm^{-3}.

At present we cannot answer the question "How low can the maximum temperature of a flare be, and what are the minimum emission measure levels of the coldest flares?" If we are to establish lower limits on emission measures and

maximum temperatures using a S XV–type detector, a substantially more sensitive detecting system will be needed. However, a system that employs a detector based on spectral lines in which the $G(T_e)$ peaks at ≈ 2–4×10^6 K (e.g., O VII, Ne IX, Mg XI) would be significantly more efficient for studies of very low temperature flare plasmas. We do not have good He-like density-sensitive lines to diagnose high-temperature flare plasmas. However, for low-temperature flares, Ne IX and in particular O VII are excellent for electron temperature, electron density, and emission measure studies (Feldman 1981). An X-ray spectrometer with detectors for the O VII, Ne IX, and Mg XI lines and their satellites, launched during a solar minimum period, would be a desirable instrument for studying properties of the coldest flares. Ironically, for studying the coldest flares, the best mission might be launched at solar minimum in order to minimize background radiation. This is in fact essential for uncollimated instruments.

We thank Mrs. Catherine A. Abbott for her assistance with the data processing. One of us (G. A. D) acknowledges support from a *Yohkoh* NASA Guest Investigator grant from the Solar Physics Branch of the Space Physics Division.

REFERENCES

Arnaud, M., & Rothenflug, R. 1985, A&AS, 60, 425
Bely-Dubau, F., Dubau, J., Faucher, P., & Gabriel, A. H. 1982a, MNRAS, 198, 239
Bely-Dubau, F., et al. 1982b, MNRAS, 201, 1155
Cornille, & Dubau, J. 1990, private communication
Culhane, J. L., et al. 1991, Sol. Phys., 136, 89
Donnelly, R. F., & Unzicker, A. 1974, NOAA Tech. Memo. ELR SEL-72
Feldman, U. 1981, Phys. Scr., 24, 681
Feldman, U., Doschek, G. A., Mariska, J. T., & Brown, C. M. 1995, ApJ, 450, 441
Feldman, U., Doschek, G. A., & McKenzie, D. L. 1984, ApJ, 276, L53
Gabriel, A. H. 1972, MNRAS, 160, 99
Garcia, H. A. 1994, Sol. Phys., 154, 275
Ogawara, Y., Takano, T., Kato, T., Kosugi, T., Tsuneta, S., Watanabe, T., Kondo, I., & Uchida, Y. 1991, Sol. Phys., 136, 1
Sterling, A. C., Doschek, G. A., & Pike, C. D. 1994, ApJ, 435, 898
Vainstein, L. A., & Safronova, U. I. 1978, At. Data Nucl. Data Tables, 21, 49
———. 1985, Phys. Scr., 31, 519
Zarro, D. M., Lemen, J. R., & Phillips, K. J. H. 1994, private communication